Available online at www.sciencedirect.com
SCIENCE DIRECT®
Precambrian Research 125 (2003) 161–178
Precambrian Research
www.elsevier.com/locate/precamres

Geochemistry and petrogenesis of a high-K calc-alkaline Dokhan Volcanic suite, South Safaga area, Egypt: the role of late Neoproterozoic crustal extension

A.M. Moghazi

Department of Geology, Faculty of Science, Alexandria University, Alexandria, Egypt

Received 5 September 2002; accepted 14 March 2003

Abstract

The South Safaga area, Central Eastern Desert of Egypt, comprises an undeformed Dokhan Volcanic suite, which is temporally and spatially associated with immature clastic sediments belonging to the Hammamat Group. Undeformed high level leucogranite intrusions and dykes have invaded these volcanic rocks whereas relatively more deformed lithologies, represented by a syn-tectonic metavolcano-sedimentary association and an I-type tonalite–granodiorite underlie them. The Dokhan Volcanic suite consists of two units: (1) a mafic unit composed of basalt, basaltic andesite, andesite, dacite and their pyroclastic equivalents, (2) a felsic unit of rhyodacite and rhyolite composition in addition to welded flow tuffs. The chemical data of the entire suite show general trends of increasing contents of incompatible elements (K_2O, Rb, Nb, Y, and Th), and decreasing contents of elements compatible with clinopyroxene, feldspars, and magnetite (e.g. MgO, $Fe_2O_3{}^*$, Al_2O_3, CaO, TiO_2, Ni, Sr, and Ba) with increasing SiO_2. Although these variations are consistent with closed system fractional crystallization processes, the slightly wide variation of Rb/Zr and La/Sm in the felsic volcanics may indicate random crustal contamination during the evolution of these rocks. Normalized trace element patterns show enrichment in LILEs (Rb, Ba, K, Th, and Ce) relative to HFSEs (Nb, Zr, P, and Ti) and are very similar to calc-alkaline subduction-related rocks from orogenic belts. However, the stratigraphic position of the Dokhan Volcanic rocks in relation to the major structural features and tectono-metamorphic events in the Eastern Desert of Egypt suggests that these rocks post-date active subduction. They were emplaced during a post-orogenic extensional collapse event that follows continental collision during late stages of the late Neoproterozoic Pan-African crustal evolution. Major and trace element arc signature of these rocks indicate partial melting of a lithospheric mantle enriched during a previous long subduction event in the Arabian–Nubian Shield. Further investigation of the regional significance of the Dokhan Volcanic rocks and their associated clastic sediments shows that the extensional episode during which these rocks were formed is a regional one.

Keywords: Neoproterozoic; Dokhan Volcanics; Geochemistry; Extension; Egypt

1. Introduction

The question of the origin of high-K and calc-alkaline rocks with an arc trace element signature is a global one (e.g. Rock, 1984; Sloman, 1989; Turner et al., 1999). It has long been recognized that there is a genetic relationship between high-K calc-alkaline magmatism and subduction zones (Peccerillo, 1985; Rogers and Hawkesworth, 1985). Trace element enrichments in large ion lithophile elements (LILE) and light rare earth elements (LREE) combined with relative depletions in the high field strength elements

E-mail address: moghazi_16@yahoo.com (A.M. Moghazi).

0301-9268/03/$ – see front matter © 2003 Elsevier Science B.V. All rights reserved.
doi:10.1016/S0301-9268(03)00110-4

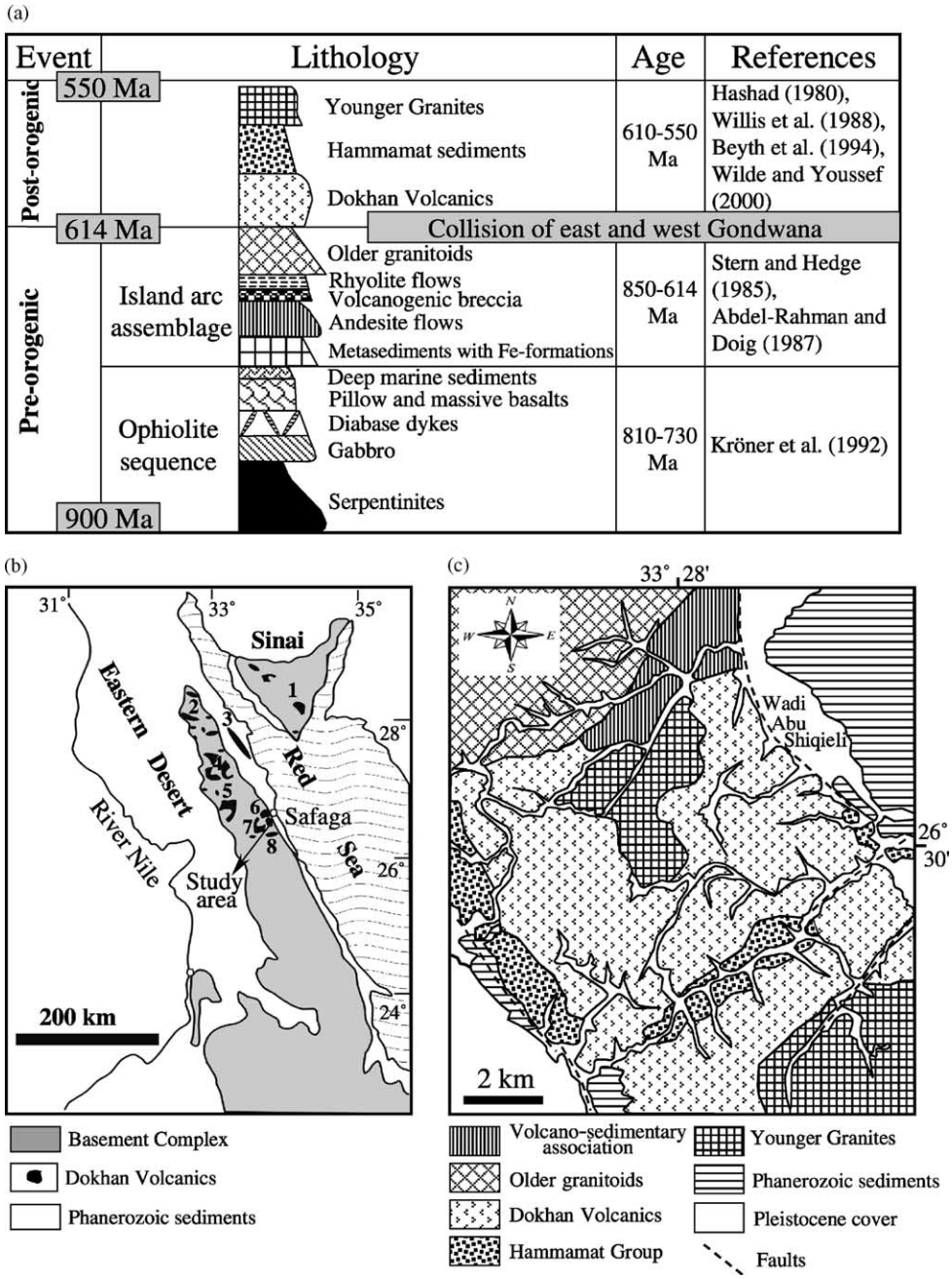

Fig. 1. (a) Lithostratigraphy and major tectonic events of the Pan-African basement complex in Egypt (modified from Stern, 1981 and Beyth et al., 1994) (see Abdel-Rahman and Doig, 1987 and Hashad, 1980). (b) A map showing the distribution of the Dokhan Volcanic rocks in northern Egypt (Geological Map of Egypt, 1987) and the location of the study area The location of the main previously studied Dokhan Volcanic occurrences are indicated by numbers as follows: (1) Wadi Kid (Moghazi, 1994), (2) El Kharaza (Abdel-Rahman, 1996), (3) G. Esh El Mellaha (El Bayoumi et al., 1997; El Sheshtawi et al., 1997), (4) G. Dokhan (Stern and Gottfried, 1986), (5) Fatira area (Ressetar and Monard, 1983; Mohamed et al., 2000), (6) G. Nuqara (Stern and Gottfried, 1986), (7) Wassif area (Heikal et al., 1980), (8) Wadi Queih (El Gaby et al., 1989). (c) Geological map of the study area (modified from Mawas, 1986).

(HFSE) are common to these arc lavas (Gill, 1981; Wilson, 1989). However, the eruption of high-K magmas with a typical arc trace element signature is recorded post-dating active subduction and occurs synchronous with uplift, extension or strike–slip motion (Sloman, 1989). The interpretations of these rocks indicate that chemical heterogenities, produced in the mantle via metasomatism, can exist for substantial periods of time after cessation of subduction (Rogers et al., 1987; Thirwall, 1988; Sloman, 1989).

The basement complex of Egypt east of the Nile, including the Eastern Desert and Sinai, is a juvenile terrane defined by Neoproterozoic Nd model ages (Stern, 2002). The most conspicuous feature of this terrane is the presence of highly deformed and metamorphosed dismembered ophiolitic suites, volcano-sedimentary associations and calc-alkaline I-type intrusive complexes. Present idea on the geotectonic evolution of these orogenic belts points to the preponderate role of convergence plate boundaries, through the formation of intra-oceanic island arc system, subsequent ocean closure, amalgamation of the arc complexes and accretion to continental crust (Vail, 1985; El Gaby et al., 1988; Kröner et al., 1988; Stern, 1994). These processes took place during the Pan-African orogenic event (Fig. 1a) between 900 and 614 Ma (Stern and Hedge, 1985; Kröner et al., 1992; Beyth et al., 1994; Stern, 1994). The terminal stage in the late Neoproterozoic crustal evolution in Egypt (between ca. 614 and 550 Ma, Fig. 1a) witnessed the emplacement of K-rich volcanic rocks (Dokhan Volcanics, El Ramly, 1972) and shallow level felsic intrusions (Younger Granites, El Gaby, 1975). These are mostly undeformed and accompanied by the deposition of molasse-type sediments (Hammamat Group, Akaad and Noweir, 1980). There is a considerable discussion over whether magmatism at this stage is related to subduction (e.g. Hassan and Hashad, 1990; El Gaby et al., 1990; Abdel-Rahman, 1996) or crustal extension (Stern et al., 1984; Stern, 1994; Fritz et al., 1996). The cornerstone of this controversy is the interpretation of geochemical data of these rocks. This paper presents new geologic and chemical data on the Dokhan Volcanic rocks of the South Safaga area, Eastern Desert, Egypt. This area is located about 30 km to the south of Port Safaga along the Red Sea coast (Fig. 1b) and just to the south of the Nuqara Dokhan Volcanic suite studied by Stern and Gottfried (1986). The aim is to integrate field and geochemical data with the structural and metamorphic history of the region in order to discriminate between the various competing models. The new data along with some published data provide additional input to this debate.

2. Geological setting

2.1. General setting and previous works

The Dokhan Volcanics are widely distributed in the Northern Eastern Desert and Sinai (Fig. 1b). Field relations indicate that the Dokhan Volcanics postdate the calc-alkaline syn-tectonic older granitoids and are predate the molasse-type Hammamat Group of sediments and the Younger Granites (El Ramly, 1972; El Shazly, 1977; Akaad and Noweir, 1980). However, other studies (Ghobrial and Lotfi, 1967; Grothaus et al., 1979; El Gaby et al., 1990) proved the presence of interfingering relationship between the Hammamat Group and the Dokhan Volcanics. SHRIMP U–Pb zircon dating (Wilde and Youssef, 2000) on two andesite samples of the Dokhan Volcanics at the type locality area at Gebel Dokhan yield a weighted $^{206}Pb/^{238}U$ ages of 593 ± 13 Ma and 602 ± 9 Ma. Rb/Sr ages of 610–560, 600–585, and 610–550 Ma have been determined for the Dokhan Volcanics, the Hammamat sediments and the Younger Granites, respectively (Stern and Hedge, 1985; Bentor, 1985; Willis et al., 1988; Beyth et al., 1994; Moghazi et al., 1998). Moreover, inspection of the clast population from the Hammamat conglomerate indicates the presence of Dokhan Volcanics and Younger Granite clasts in these sediments (Ries et al., 1983). These field and geochronological data indicate that the three rock units are broadly penecontemporaneous.

The Dokhan Volcanics have been investigated petrologically and geochemically since the early 20th century by many authors (viz. Hume, 1935; Schürmann, 1966; Basta et al., 1980; Akaad and Noweir, 1980; Ressetar and Monard, 1983; Stern et al., 1984; Stern and Gottfried, 1986; Ragab, 1987; El Gaby et al., 1989; Abdel-Rahman, 1996; Mohamed et al., 2000). Many of these studies show the high-K and calc-alkaline nature of the Dokhan Volcanics and provide evidence for the operation of fractional crystallization and crustal contamination in the evolution

of these rocks. However, the geotectonic interpretation of the Dokhan Volcanics has been highly debated with models centered around three main settings: (1) anorogenic setting: intra-continental rift model similar to the Oslo rift system in Norway (Stern et al., 1984, 1988; Stern and Gottfried, 1986); (2) orogenic setting: active continental margin (Basta et al., 1980; Ragab, 1987; El Gaby et al., 1988, 1989; Abdel-Rahman, 1996; El Bayoumi et al., 1997; El Sheshtawi et al., 1997); and (3) transitional setting: transitional between compressional and extensional settings (Ressetar and Monard, 1983; Mohamed et al., 2000). This paper seeks to address this debate.

2.2. Field observations

Various volcanic and plutonic rocks of Neoproterozoic age are exposed in the study area (Fig. 1c): metavolcano-sedimentary association, syn-tectonic older granitoids, Dokhan Volcanics, Hammamat sediments, and younger leucogranites. The metavolcano-sedimentary association represents the oldest unit, which occupies a small area (about 8 km × 2 km) to the northeast of the study area. It consists of a deformed succession of mafic to intermediate volcanic rocks and volcaniclastics with intercalations of pelitic sediments (greywackes and siltstone) that have been regionally metamorphosed in the greenschist facies. The syn-tectonic older granitoids (mainly tonalite and granodiorite) crop out in the northwestern part and extends to the north and west beyond the limits of the study area. They intrude the volcano-sedimentary association along a sharp contact with local development of hornblende–hornfels in the volcano-sedimentary association. This granite suite is homogeneous, coarse- to medium-grained, light gray and encloses few mafic enclaves. In places, it is sheared and foliated.

The Dokhan Volcanics in the study area, about 1.3 km thick, occupy a vast area (~90 km^2) forming moderately high mountaineous ridges with rough topography and crenulated peaks. They consist of varicolored alternating successions of lava flows of mafic and felsic composition interlayered with pyroclastic rocks. Repeated eruptions of the mafic to felsic volcanic materials locally produced layered structures. This sequence is similar to that at Gabal El Kharaza (Northern Eastern Desert) reported by Abdel-Rahman (1996) and differs from the Nuqara Dokhan Volcanics (west of Safaga) that consist of lower andesitic section and upper felsic section (Stern and Gottfried, 1986). Field relations show that the Dokhan Volcanics in the study area overlie the syn-tectonic older granites, but are intruded by the younger leucogranite and by dykes. They are also overlain by local occurrences of molasse-type Hammamat sediments (Fig. 1c), which consist of conglomerate, greywacke and siltstone. In some places, particularly in the southern part of the study area, the Dokhan Volcanics and the Hammamat sediments interfinger.

3. Petrography

Based on mineralogical composition and geochemical data (see below), the investigated volcanic suite can be divided into two units, namely: mafic and felsic units.

3.1. The mafic volcanics

The mafic volcanic rocks are basalt, basaltic andesite, andesite and dacite. They exhibit black, green and gray colors and are texturally porphyritic (with plagioclase phenocrysts up to 8 mm × 3 mm). Some of the porphyrites are purple similar to the classical imperial porphyry unit of Gabal Dokhan described by Basta et al. (1980). The basalts are of limited distribution and contain up to 15 modal percent phenocrysts of plagioclase, augite and rare magnetite microphenocrysts. Sub-ophitic and amygdaloidal textures are occasionally recorded. The plagioclase phenocrysts (the dominant phenocryst) are labradorite ($An_{55–60}$) in the form of subhedral-zoned crystals. Augite phenocrysts in the form of equant crystals (0.5–0.3 mm) are sometimes pseudomorphosed by amphibole. The groundmass is fine-grained to microcrystalline consisting of plagioclase, augite and magnetite together with minor secondary epidote, and chlorite. Accessory apatite, as inclusions in plagioclase and augite, is also reported. The basaltic andesites and andesites show typical flow structure defined by the parallel arrangement of the plagioclase phenocrysts. They contain about 20–25 modal percent phenocrysts of plagioclase ($An_{40–50}$), hornblende, and augite in an intergranular or hyalopilitic matrix dominated by hornblende and plagioclase. Chlorite, actinolite, and epidote are alteration products whereas apatite and magnetite are the common acces-

sory mineral. Amygdaloidal varieties of the andesites are common where the filling minerals include natrolite, calcite, quartz and chalcedony. Dacite is mainly made up of plagioclase feldspar ($An_{15–20}$), quartz, alkali feldspar and chloritized hornblende microphenocrysts set in a microcrystalline matrix consisting of a dense mat of quartz and feldspars. Apatite, magnetite and occasionally ilmenite are accessory minerals.

3.2. The felsic volcanics

The acidic volcanic rocks are mainly rhyodacites and rhyolites in addition to welded tuffs (ignimbrite), which exhibit brown, pink and red colors. They are vesicle-free and flow banded with a conspicuous porphyritic texture in which coarse-grained feldspar phenocrysts (up to 5 mm × 2 mm) occur in a microgranular to vitrophyric groundmass. The main constituent minerals are: K-feldspar, quartz, plagioclase feldspar ($An_{10–18}$) and some biotite. Zircon, apatite, magnetite, and ilmenite are accessory minerals. Additionally, secondaries occur as late-formed chlorite and calcite. Ash flow tuffs (ignimbrite) are thin-bedded rhyolitic tuffs of brownish color. They consist of a mixture of lithic and crystal fragments together with devitrified acid volcanic glass having a flow-like texture of alternating fine-grained and microcrystalline bands. These bands are curved and form parallel streaks and strings. Some samples contain phenocrysts of quartz and feldspar set in a felsic vitrophyric groundmass. In addition, pyroclastic rocks represented by agglomerates, lapilli tuffs, and crystal-lithic tuffs occur. The agglomerates are massive and formed of elliptical and poorly sorted andesite and dacite fragments embedded in a fine-grained tuffaceous matrix. Lapilli and crystal-lithic tuffs are composed of rock fragments (up to 2 mm across) and crystal fragments (up to 0.7 mm long) of plagioclase, quartz and hornblende set in a tuffaceous cryptofelsitic matrix. The matrix is primarily composed of quartz, feldspar, epidote, magnetite, and ilmenite with few streaks of chlorite, biotite and calcite.

4. Geochemistry

4.1. Sample set and analytical techniques

Twenty-six representative samples covering the different volcanic rocks were petrographically selected for chemical analyses. Major and trace elements were determined by X-ray fluorescence spectrometry technique using a Philips PW 2400 instrument with an end window Rh tube at the Geology Institute, University of Oslo, Norway. Major elements were determined on fused $LiBO_4$ disks while trace element analyses were performed on pressed powder pellets. Loss on ignition (LOI) was determined by heating powdered samples for about 1 h at 1000 °C. Analytical precision based on duplicate analyses are expressed in terms of relative percentages and are found to vary

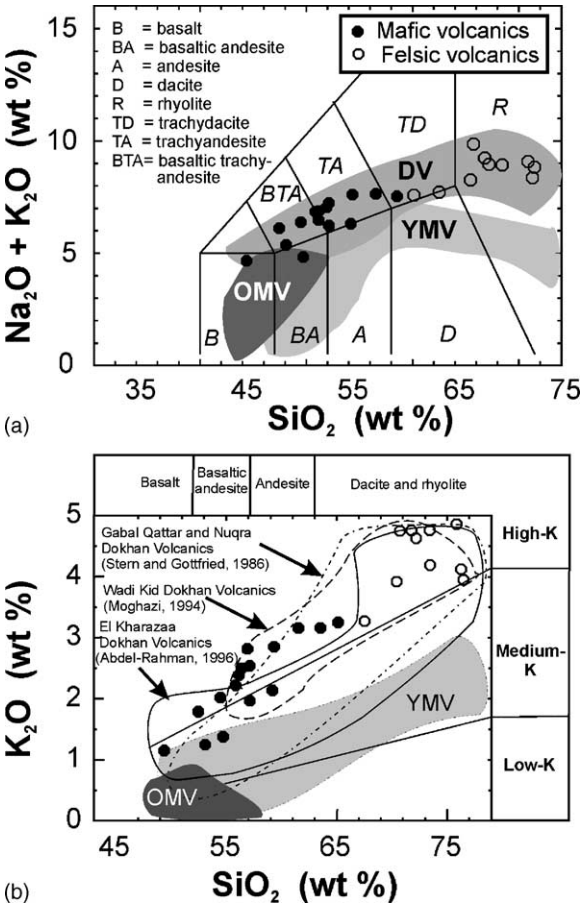

Fig. 2. (a) SiO_2 vs. $Na_2O + K_2O$ (Le Bas et al., 1986) and (b) SiO_2 vs. K_2O (Peccerillo and Taylor, 1976) diagrams showing geochemical classification of the South Safaga Dokhan Volcanic rocks: shown for comparison the fields of ophiolitic older metavolcanics (OMV), island arc younger metavolcanics (YMV) using data from Stern (1981). Also shown the fields of Dokhan Volcanic rocks (DV) from different areas in Egypt.

Table 1
Chemical data (major and trace elements) of the South Safaga Dokhan-type volcanic rocks

	SS2 (A)	SS5 (A)	SS6 (B)	SS7 (BA)	SS10 (BA)	SS11 (BA)	SS12a (A)	SS12b (D)	SS14 (A)	SS15 (A)	SS18 (A)	SS19 (A)	SS20 (A)
Major elements (wt.%)													
SiO_2	57.13	59.18	49.38	53.08	52.46	54.72	61.52	63.53	56.15	56.90	56.15	57.11	59.32
TiO_2	1.15	0.96	1.79	1.59	1.68	1.24	1.01	0.77	1.22	1.32	1.43	1.02	1.12
Al_2O_3	17.41	16.97	16.81	16.65	16.72	16.74	17.03	15.53	17.44	16.65	17.51	17.15	16.44
Fe_2O_3*	7.16	6.17	8.94	8.62	7.65	8.52	5.26	5.68	7.59	7.16	6.37	6.77	6.13
MnO	0.15	0.15	0.15	0.13	0.13	0.16	0.11	0.13	0.14	0.15	0.18	0.14	0.11
MgO	2.95	2.69	8.45	4.95	5.51	6.38	2.05	1.47	3.91	3.51	2.84	3.13	3.07
CaO	5.44	5.52	7.76	6.82	7.21	5.59	4.15	3.59	5.22	5.65	5.08	5.44	4.62
Na_2O	4.26	4.17	3.51	4.12	4.32	3.45	4.48	4.37	4.03	4.22	4.47	4.69	4.76
K_2O	1.97	2.14	1.15	1.25	1.79	1.38	3.16	3.16	2.45	2.82	2.39	2.54	2.85
P_2O_5	0.24	0.28	0.27	0.35	0.43	0.21	0.20	0.12	0.21	0.35	0.35	0.27	0.19
LOI	1.64	1.41	1.65	2.25	1.41	1.45	0.82	0.70	1.55	1.16	2.10	1.52	0.76
Sum	99.50	99.64	99.86	99.81	99.31	99.84	99.79	99.05	99.91	99.89	98.87	99.78	99.37
Mg#	45	46	65	53	59	60	44	34	51	49	47	48	50
$Na_2O + K_2O$	6.23	6.31	4.66	5.37	6.11	4.83	7.64	7.53	6.48	7.04	6.86	7.23	7.61
Na_2O/K_2O	2.16	1.95	3.05	3.30	2.41	2.50	1.42	1.38	1.64	1.50	1.87	1.85	1.67
FeO*/MgO	2.18	2.06	0.95	1.57	1.25	1.20	2.31	3.48	1.75	1.84	2.02	1.95	1.80
Trace elements (ppm)													
Cr	124	157	250	215	128	254	56	10	120	183	90	150	106
Ni	47	66	180	126	96	112	15	4	55	50	73	39	71
Co	22	23	35	27	31	38	17	11	30	28	29	21	20
V	190	135	280	265	250	242	166	150	215	140	103	127	178
Pb	17	21	18	14	15	17	19	28	19	18	15	18	20
Zn	17	21	18	14	15	17	62	110	19	18	15	18	85
Rb	65	51	32	35	45	37	76	85	62	72	54	67	64
Ba	678	914	602	543	643	711	712	868	771	715	940	551	654
Sr	690	773	940	745	791	620	415	385	930	892	810	363	335
Nb	10	8	5	7	8	4	8	15	5	5	8	11	9
Zr	195	190	157	203	190	153	240	308	145	230	227	160	285
Y	21	20	19	20	26	18	29	35	22	21	19	24	27
Th	5	6	4	4	3	5	6	6	8	5	6	4	5
U	2	nd	2	2	2	2	3	4	2	2	2	nd	3
Zr/Y	9	10	8	10	7	9	8	9	7	11	12	7	11
K/Rb	252	348	298	296	330	310	345	309	328	325	367	315	370
Rb/Sr	0.06	0.07	0.05	0.05	0.06	0.06	0.18	0.22	0.04	0.04	0.05	0.16	0.15
Rb/Ba	0.06	0.06	0.08	0.06	0.07	0.05	0.11	0.10	0.05	0.05	0.04	0.11	0.07

Table 1 (*Continued*)

	SS22 (BA)	SS23 (BA)	SS26 (RD)	SS27 (RD)	SS28 (R)	SS30 (R)	SS33 (R)	SS34 (RD)	SS35 (RD)	SS38 (R)	SS42 (R)	SS48 (R)	SS49 (R)
Major elements (wt.%)													
SiO_2	54.47	55.84	70.43	70.73	73.42	75.85	76.27	65.13	67.52	72.18	71.78	73.45	76.47
TiO_2	1.65	1.72	0.33	0.28	0.32	0.26	0.18	0.55	0.39	0.24	0.30	0.25	0.31
Al_2O_3	16.39	17.13	14.77	13.57	13.33	12.85	12.45	15.55	15.64	13.65	13.26	13.03	12.06
$Fe_2O_3^*$	8.63	7.22	2.22	2.67	1.20	1.36	1.25	3.91	3.45	2.51	2.65	1.32	1.44
MnO	0.21	0.15	0.08	0.10	0.05	0.03	0.05	0.09	0.11	0.10	0.05	0.08	0.03
MgO	3.97	3.03	0.62	0.41	0.37	0.25	0.13	1.36	0.87	0.48	0.31	0.29	0.17
CaO	5.85	4.42	2.07	1.04	1.14	0.70	0.82	3.32	2.47	0.89	0.95	0.79	0.57
Na_2O	4.36	4.63	4.34	5.11	4.17	4.22	4.24	4.33	4.45	4.33	4.48	4.73	4.88
K_2O	2.02	2.22	3.92	4.75	4.76	4.86	4.12	3.25	3.27	4.63	4.76	4.19	3.95
P_2O_5	0.48	0.50	0.08	0.04	0.05	0.03	0.05	0.16	0.13	0.03	0.02	0.05	0.03
LOI	0.79	2.33	0.72	0.54	0.65	0.46	0.57	0.62	1.46	0.58	0.46	0.67	0.68
Sum	98.82	99.19	99.58	99.24	99.46	100.87	100.13	98.27	99.76	99.62	99.02	98.85	100.59
Mg#	48	45	36	23	38	27	17	41	33	27	19	30	19
$Na_2O + K_2O$	6.38	6.85	8.26	9.86	8.93	9.08	8.36	7.58	7.72	8.96	9.24	8.92	8.83
Na_2O/K_2O	2.16	2.09	1.11	1.08	0.88	0.87	1.03	1.33	1.36	0.94	0.94	1.13	1.24
FeO^*/MgO	1.96	2.14	3.22	5.86	2.92	4.89	8.65	2.59	3.57	4.71	7.69	4.10	7.62
Trace elements (ppm)													
Cr	184	175	16	10	40	15	8	64	40	33	16	7	20
Ni	95	99	6	2	22	8	3	20	8	2	2	3	6
Co	25	22	7	5	8	4	3	15	7	4	3	3	3
V	115	232	25	15	12	9	5	68	64	9	7	5	7
Pb	10	13	7	8	22	15	9	27	18	17	27	16	12
Zn	10	13	23	10	73	64	14	92	45	55	37	21	34
Rb	57	55	121	138	132	110	160	90	81	112	117	120	140
Ba	842	782	880	585	686	420	618	1075	881	851	604	592	342
Sr	646	620	295	96	169	152	120	280	391	38	55	120	65
Nb	9	9	9	22	13	15	15	10	11	17	14	12	14
Zr	146	150	242	266	217	228	270	295	272	305	400	240	212
Y	20	18	38	45	42	35	40	32	40	35	33	37	52
Th	4	5	9	12	10	11	11	8	8	12	13	10	9
U	3	2	5	6	7	7	6	4	5	7	7	6	5
Zr/Y	7	8	6	6	5	7	7	9	7	9	12	6	4
K/Rb	294	335	269	286	299	367	266	300	335	343	338	290	294
Rb/Sr	0.09	0.09	0.41	1.44	0.78	0.72	1.33	0.32	0.21	2.95	2.13	1.00	2.15
Rb/Ba	0.07	0.07	0.14	0.24	0.19	0.26	0.26	0.08	0.09	0.13	0.19	0.20	0.41

$Fe_2O_3^*$: total Fe as Fe_2O_3, nd: below detection limit, B: basalt, BA: basaltic andesite, A: andesite, D: dacite, RD: rhyodacite, R: rhyolite.

Table 2
Rare earth element data of the South Safaga Dokhan-type volcanic rocks

	SS6 (B)	SS11 (BA)	SS19 (A)	SS20 (A)	SS27 (RD)	SS48 (R)	SS49 (R)
La	18.81	23.30	27.33	28.34	54.10	43.01	36.29
Ce	40.35	50.82	60.14	61.04	96.58	78.06	72.58
Pr	4.47	5.59	7.17	7.95	12.54	6.83	10.30
Nd	17.58	20.79	30.02	31.47	48.27	22.85	34.83
Sm	4.70	5.96	6.50	6.83	11.46	4.82	7.39
Eu	1.34	1.57	1.72	1.85	1.79	0.69	1.42
Gd	4.20	4.93	5.49	5.60	9.91	5.82	6.72
Tb	0.67	0.75	0.78	0.84	1.40	0.90	1.01
Dy	3.53	3.47	4.82	4.37	6.79	4.26	5.94
Ho	0.67	0.62	0.73	0.73	1.51	0.90	1.34
Er	1.57	1.46	1.70	1.85	3.90	2.58	3.58
Tm	0.19	0.17	0.25	0.26	0.49	0.39	0.56
Yb	1.29	1.06	1.96	1.87	2.91	2.24	3.02
Lu	0.18	0.16	0.24	0.27	0.50	0.28	0.34
$\sum$REE	100	121	149	153	252	174	185
(Ce/Yb)*n*	8.1	12.4	8.0	8.5	8.6	9.0	6.2
(La/Sm)*n*	2.5	2.5	2.6	2.6	3.0	5.6	3.1
(Gd/Yb)*n*	2.6	3.8	2.3	2.4	2.8	2.1	1.8
Eu/Eu*	0.92	0.89	0.88	0.91	0.51	0.40	0.62

B: basalt, BA: basaltic andesite, A: andesite, RD: rhyodacite, R: rhyolite.

from ±0.25 to ±2.5% for major elements and from ±3 to ±10% for trace elements. Rare earth element contents in seven samples were determined by inductively coupled plasma-mass spectrometry (ICP-MS) at the ACME Analytical Laboratories Ltd., Canada. Precision (in relative percentages) based on duplicate analyses are in the range ±4.5 and ±13. The chemical data of the analyzed samples are shown in Tables 1 and 2.

4.2. Classification and comparison with other volcanic occurrences in Egypt

According to the SiO_2 versus Na_2O+K_2O diagram recommended by the International Union of Geological Sciences (IUGS) for the classification of volcanic rocks (Le Bas et al., 1986), the investigated volcanic rocks have a wide range of SiO_2 (49–77%) ranging from mafic (basalt, basaltic andesite, andesite and dacite) to felsic (rhyodacite and rhyolite) members (Fig. 2a). Comparison of the studied volcanic rocks with different types of volcanic rocks in the basement complex of Egypt, using published data, confirms earlier observations (Stern et al., 1984; El Gaby et al., 1988; Mohamed et al., 2000) that the Dokhan Volcanics differ from the older stratigraphic volcanics even for rocks with similar SiO_2 contents. The SiO_2 versus K_2O diagram (Fig. 2b) of Peccerillo and Taylor (1976) shows the fields of ophiolitic metavolcanics (OMV), island arc metavolcanics (YMV) and Dokhan Volcanics (DV). The ophiolitic metavolcanics are distinctly low-K basalts and basaltic andesites. The island arc metavolcanics cover a wide range of SiO_2 similar to the Dokhan Volcanics, but are distinct in being low- to medium-K. The investigated volcanic suite typically resembles the Dokhan Volcanics elsewhere in the Eastern Desert and Sinai with the mafic varieties are medium- to high-K and the felsic varieties are high-K (Fig. 2b).

4.3. Major and trace element variations

The mafic volcanics (49–63% SiO_2) are silica saturated. Their Mg# (100 Mg/(Mg + Fe^{2+}), with Fe^{3+}/Fe^{2+} standardized to 0.2) range from 65 to 34 (Table 1) suggesting that these rocks are not primary mantle-derived melts. Samples with high Mg# (>60) characterize rocks with the lowest Nb and Zr and the highest Cr and Ni. Overall, they are characterized by rather high contents and wide range

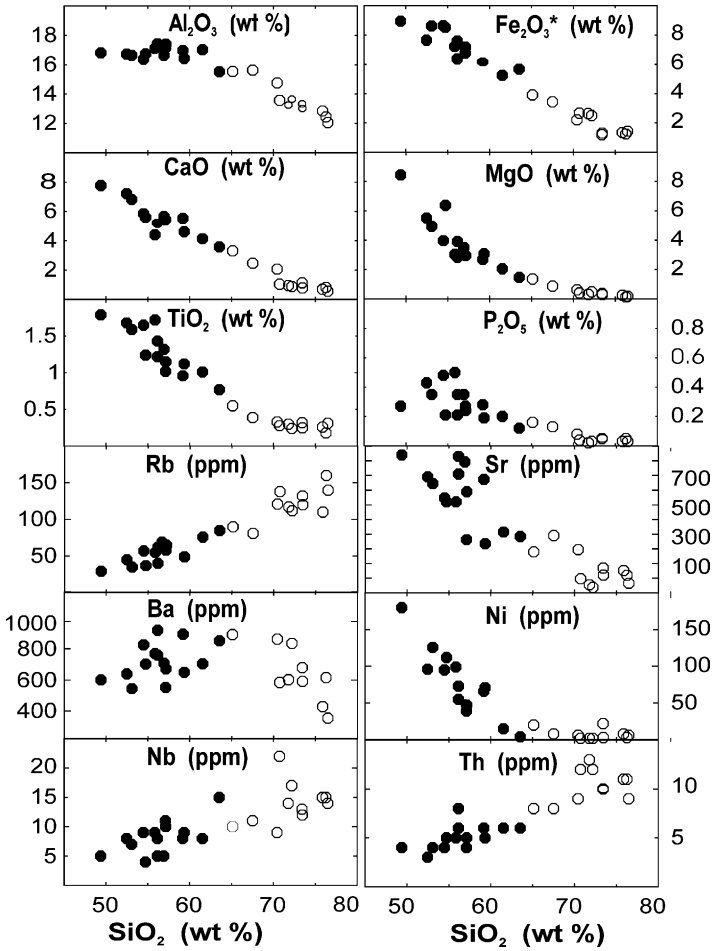

Fig. 3. Harker variation diagrams of some major and trace elements of the South Safaga Dokhan Volcanic rocks. Symbols as in Fig. 2.

of Al_2O_3 (15.5–17.5 wt.%), TiO_2 (0.8–1.8 wt.%), $Na_2O + K_2O$ (4.7–7.6%), Na_2O/K_2O (1.4–3.3), P_2O_5 (0.2–0.5 wt.%), Rb (32–85 ppm), Ba (543–940 ppm), Sr (335–940 ppm), Zr (145–308 ppm), and Nb (5–15 ppm). The felsic volcanics (65–76% SiO_2) are marked by relatively high $Na_2O + K_2O$ (7.6–9.8%), Rb (81–160 ppm), Zr (217–400 ppm), Y (32–52 ppm), and Nb (9–22 ppm) and low Al_2O_3 (12.1–15.6%), MgO (0.13–1.36%), CaO (0.6–3.32%), and Sr (38–391 ppm).

Silica variation diagrams of major and trace element are illustrated in Fig. 3. The rocks of the entire volcanic suite define strongly correlated and continuous variation trends. MgO, Fe_2O_3 (total), TiO_2, MgO, P_2O_5, and CaO decrease with increasing SiO_2 whereas K_2O and $Na_2O + K_2O$ contents increase (Fig. 2). Al_2O_3 remains nearly unchanged with increasing silica during crystallization of the mafic volcanic rocks, but decreases later during the crystallization of the felsic varieties. Rubidium, Nb, and Th abundances increase systematically with increasing SiO_2 whereas Sr and Ni decrease. Barium abundances show much less coherent variation than is observed for K_2O and Rb. The mafic volcanic samples have Ba concentrations showing a positive linear correlation with SiO_2 in contrast with the acidic volcanic rocks.

All lithological units are enriched in light relative to heavy REE (HREE; Fig. 4). REE patterns of the mafic volcanics are relatively steep ($(Ce/Yb)n = 8–12$) with very small negative Eu anomalies ($Eu/Eu^* =$

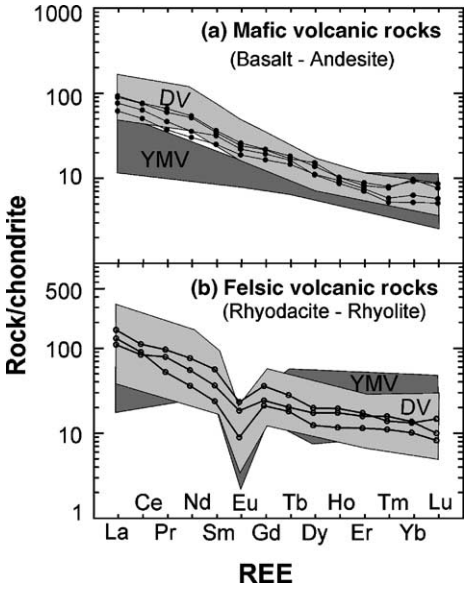

Fig. 4. Chondrite-normalized REE plots (Sun, 1982) of the South Safaga mafic and felsic Dokhan Volcanic rocks. The fields labeled YMV and DV as in Fig. 2.

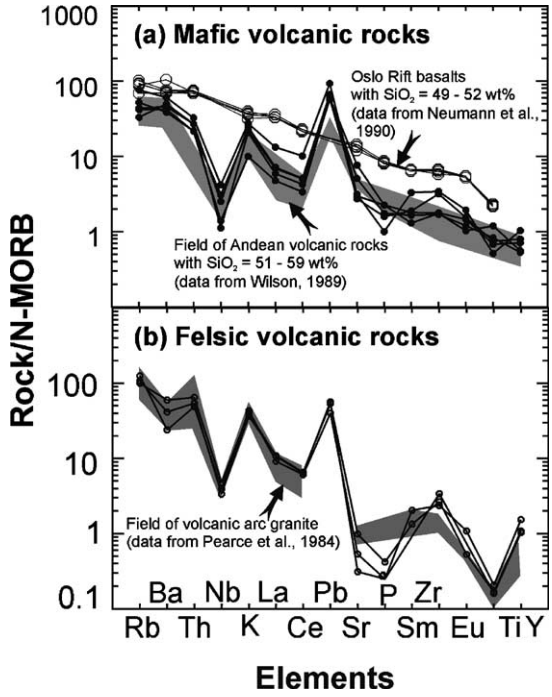

Fig. 5. N-MORB-normalized trace element plots for the South Safaga mafic and felsic Dokhan Volcanic rocks; shown for comparison the fields of Andean arc volcanics and Oslo Rift basalts (a) and Chile arc granite (b). Normalization values are from Sun and McDonough (1989).

0.92–0.88). The less-evolved basaltic rocks have the lowest REE contents (100 ppm) and LREE/HREE ratio (Ce/Yb)$n = 8$), which increase in the basaltic andesites ((Ce/Yb)$n = 12$). The andesites have relatively moderate REE contents (149–153 ppm) and patterns very similar to those of basalt and basaltic andesite (Table 2 and Fig. 4). The felsic volcanics are characterized by higher total REE contents (174–252 ppm), less fractionated patterns ((Ce/Yb)$n = 6.2$–9), which are steeply sloping from La to Sm and gently sloping from Gd to Yb ((Gd/Yb)$n = 1.8$–2.8) and have a pronounced negative Eu-anomaly (Eu/Eu$^* = 0.4$–0.6). Compared to island arc metavolcanics (YMV) and Dokhan Volcanics (DV) from various localities in the Eastern Desert and Sinai, the REE patterns of the investigated Dokhan Volcanics are very similar to those of the other Dokhan Volcanics in the Eastern Desert and Sinai (Fig. 4).

Relative to normal mid-ocean ridge basalts (N-MORB), the studied volcanic rocks (Fig. 5) show: enrichment in the strongly incompatible LILE such as Rb, Ba, and K; strong depletion in Nb relative to K and Th; enrichment in Pb over Ce; and LREE enrichment (La and Ce) over HREE and Y, which show abundances similar to those of N-MORB. The overall patterns of the felsic volcanic rocks are broadly similar to those of the mafic volcanics in terms of having negative Nb anomalies and positive Pb anomalies. However, they are distinguished by far more LILE enrichment. Additionally, the felsic volcanics possess negative anomalies for Ba, Sr, P, and Ti. Such anomalies may be attributed to fractionation of feldspars (for Ba and Sr depletion), apatite (for P depletion) and Fe–Ti oxides (for Ti depletion).

5. Discussion

5.1. Tectonic setting

The trace elements data of the mafic volcanic rocks along with those for the Dokhan Volcanics from previous studies are plotted on a series of tectonic

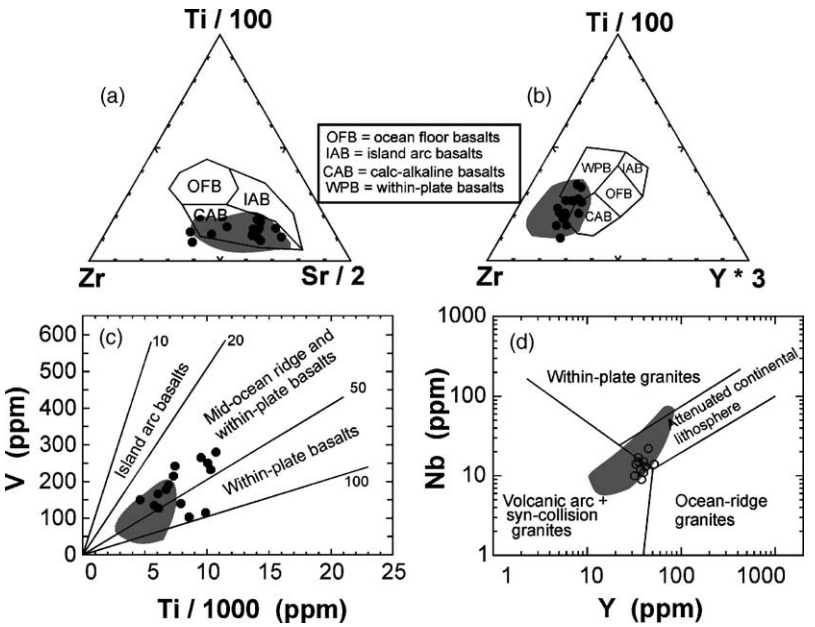

Fig. 6. Tectonic discrimination diagrams for the South Safaga Dokhan Volcanic rocks and other Dokhan Volcanic occurrences (shaded area) according to Fig. 2: (a) Zr–Ti–Sr diagram (Pearce and Cann, 1973), (b) Zr–Ti–Y diagram (Pearce and Cann, 1973), (c) Ti vs. V diagram of Shervais (1982), and (d) Nb vs. Y (Pearce et al., 1984). Symbols as in Fig. 2.

discrimination diagrams (Fig. 6). On the Zr–Ti–Sr ternary diagram (Fig. 6a) they show geochemical characteristics of calc-alkaline rocks emplaced in convergent plate margins but on other diagrams such as Zr–Ti–Sr and Ti versus V diagrams (Fig. 6b and c), they are similar to within-plate basalts. The felsic volcanic rocks plot in the fields of volcanic arc and within-plate granites (Fig. 6d). Accordingly, the Dokhan Volcanics have geochemical characteristics of both subduction-related and within-plate settings. This was previously noted by many authors and has led to a debate on the convergent margin versus within-plate geotectonic setting for these lavas.

Because one of the primary objectives of this study is to determine the tectonic setting for the Dokhan Volcanic rocks, previous tectonic models will be discussed in the light of major geochemical features and geodynamic events (structural and tectono-metamorphic) in order to explain their significance and relationship to the emplacement of the Dokhan Volcanics in Egypt.

5.1.1. Subduction-related model

Although the Dokhan Volcanics are geochemically compatible with an active continental margin setting similar to the Andean volcanic rocks in western America (Fig. 5), there is some regional geodynamic evidence that supports the cessation of subduction processes before their eruption. These are as follows.

(1) Based on a detailed structural study of the Eastern Desert of Egypt, Greiling et al. (1994) discusses collision ending at 615–600 Ma and extensional collapse occurred within the 600–575 Ma time span followed by transpressional tectonism along major shear zones until 530 Ma. This is supported by geological and geochronological studies carried out at different parts in the Eastern Desert of Egypt. These studies have documented two tectono-metamorphic events in the Neoproterzoic evolution of Egypt. The first tectono-metamorphic event (between ca. 700 and 720 Ma) has been considered to represent the age of ophiolite obduction and island arc terrane accretion (Kröner et al., 1994; Harms et al., 1994; Stern, 1994, 2002). The second tectono-metamorphic event (between ca. 620 and 650 Ma) has been interpreted as a probable collisional stage during which the accreted juvenile terranes attached to the East Saharan Craton

(Schandelmeier et al., 1987; Kröner et al., 1994; Sultan et al., 1994; Finger and Helmy, 1998). The undeformed nature of the Dokhan Volcanics and their emplacement ages (610–560 Ma, Fig. 1a), which post-date the main collisional stage, indicate that these rocks are post-orogenic.

(2) The Younger Granite intrusions in Egypt are massive and undeformed post-orogenic granites with typical A-type characteristics (Stern and Gottfried, 1986; Sylvester, 1989; Moghazi, 1999, 2002). The reported ages for the A-type granites vary from 610 to 550 Ma, very similar to those (610–560 Ma) of the spatially associated Dokhan Volcanics. If the Dokhan Volcanics are subduction-related, this means that two different magma types of different tectonic environments were formed at the same time span, which is difficult to imagine. Also, the synchronous timing of the Dokhan Volcanics and the A-type granites with the major ca. 630–540 Ma Najd strike–slip fault systems in the Arabian–Nubian Shield (Fleck et al., 1976; Stacey and Agar, 1985) is difficult to elucidate with a subduction-related tectonic regime.

(3) The predominance of dyke swarms of the same age as the Dokhan Volcanics (Stern et al., 1984; Stern and Voegeli, 1987) as well as the synchronous timing of the Dokhan Volcanic rocks with some ring complexes in the northern part of the Eastern Desert (i.e. the Wadi Dib ring complex in northern Egypt dated at 578 Ma; Frisch and Abdel-Rahman, 1999) indicate the prevalence of extensional tectonics during their formation.

(4) Exhumation of metamorphic core complexes and molasse basin formation, at about 600–580 Ma (Willis et al., 1988; Fritz et al., 1996) also indicate that extensional tectonics were active during the Dokhan Volcanics formation.

5.1.2. Continental rifting model

Ressetar and Monard (1983) described the tectonic setting of the Dokhan Volcanics in the Fatira–Safaga area as transitional between compressional and extensional regimes. Stern et al. (1984, 1988), Stern and Gottfried (1986) and Willis et al. (1988) regard the wide distribution of molasse-type sediments (Hammamat Group) together with bimodal volcanic rocks (Dokhan Volcanics) and high level granite intrusions (Younger Granites) in the Egyptian basement complex as evidence of strong crustal extension in an anorogenic rift-related environment similar to the Oslo Rift in Norway. However, there are major objections to the formation of the these rock units in true anorogenic rift-related settings; these are as follows.

(1) Despite the presence of molasse-type sediments with red beds, which characterize anorogenic settings, these sediments show evidence for deposition as alluvial fan and braided stream deposits in isolated intermontane basins with local volcanic provenance (Francis, 1972; Grothaus et al., 1979). This may reflect vertical tectonics, which have resulted in uplift of crustal blocks and rapid deposition of immature detritus into adjacent local basins. Furthermore, bimodal magmatic associations cannot be used as unequivocal evidence of anorogenic rifting, a point well illustrated by the strongly bimodal magmatic assemblage in arc lavas of North Island, New Zealand (Hamilton, 1988).

(2) Geochemically, basalts from the Oslo rift have major and trace element contents similar to those of ocean island basalts (OIB), supporting the involvement of asthenospheric mantle in their origin (Neumann et al., 1990). However, trace element abundances in the Dokhan Volcanics characterize rocks derived from enriched subcontinental lithospheric mantle (Fig. 5) and rule out asthenospheric mantle source in true continental rift environments.

5.1.3. Extensional collapse (the preferred model)

As mentioned above, there is no tectonic evidence indicating that subduction of oceanic lithosphere was contemporaneous with the emplacement of the Dokhan Volcanics. The least evolved member of the studied volcanic suite is basaltic in composition (SiO_2 = 49 wt.%; MgO = 8.5 wt.%), which indicates partial melting of mantle material. N-MORB normalized spidergrams (Fig. 5) indicate that these mafic rocks originated from a section of the mantle enriched by subduction. Thus, a consistent model of the Dokhan Volcanic magmatism must explain their subduction-related chemical signature and their emplacement after final ocean closure and continental collision. This can be viewed in a model of extensional

collapse that follows continental collision and controlled mainly by lithospheric delamination and slab breakoff (passive rifting) and not by rifting controlled by the ascent of the asthenosphere (active rifting) as in the Oslo rift in Norway. The extensional collapse model has been discussed and documented in several areas (e.g. Bird, 1979; Dewey, 1984; Sacks and Secor, 1990; Davies and von Blanckenburg, 1995; Turner et al., 1999; Atherton and Ghani, 2002). In this model, as mentioned by Sacks and Secor (1990) the weight of the downgoing slab, during continental collision, may lead to extensional shearing in the descending plate (slab breakoff, Davies and von Blanckenburg, 1995) and finally to its separation from the overlying lighter crust along normal-sense shear zone. During these processes, the continental crust attached to the lower plate may undergo an episode of extensional tectonics (Sacks and Secor, 1990).

The generation of the Dokhan Volcanic magma can thus be regarded as a consequence of continental collision between the juvenile crust of the Arabian–Nubian Shield and the Saharan Craton to the west (Fig. 7). In such circumstances, slab breakoff and lithospheric delamination are natural consequences of continental collision (Davies and von Blanckenburg, 1995). The hot asthenosphere will rise through the break (Fig. 7) in a manner similar to a plume impinging on lithosphere (Atherton and Ghani, 2002). The lithosphere is heated and melted by conduction as the asthenosphere impinges its base (Fig. 7). The lithospheric mantle involved could be the perisphere that can be chemically isolated from the underlying convecting mantle. This part of lithosphere may have obtained unique trace element characteristics owing to its interaction with fluids and melts driven off from the subducting slab during previous long subduction events (i.e. between 900 and 620 Ma; Stern, 1994) in the Arabian–Nubian Shield. Expected melts, according to Davies and von Blanckenburg (1995) could be alkaline to ultrapotassic for small degrees melt or calc-alkaline from slightly higher degree melting. The calc-alkaline nature of the Dokhan Volcanics can be explained by high degree partial melting.

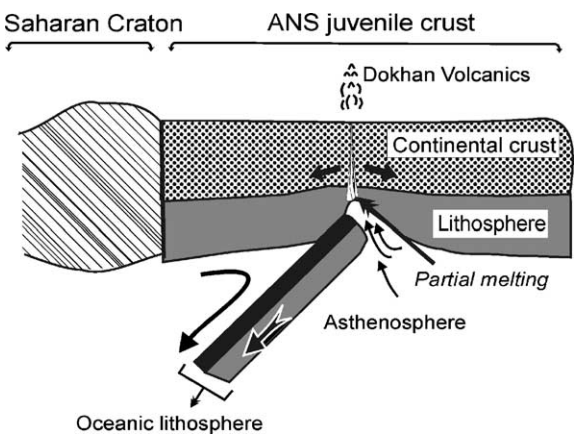

Fig. 7. Cartoon showing the generation of the Dokhan Volcanic magma as a consequence of slab breakoff on collision of the Arabian–Nubian Shield juvenile crust and the Saharan Craton. Hot asthenosphere impinges on the base of mantle lithosphere causing its partial melting and produce enriched basaltic magma (modified after Davies and von Blanckenburg, 1995).

Although this model needs to be evaluated structurally, it seems to be the most plausible for the stratigraphic position and geochemical composition of the Dokhan Volcanics.

5.2. Petrogenesis

It has been previously argued that the evolved Dokhan Volcanic rocks (andesites, dacites and rhyolites), at many areas in the Eastern Desert of Egypt, were generated from more primitive basaltic precursors by crystal fractionation (Stern and Gottfried, 1986; Abdel-Rahman, 1996; Mohamed et al., 2000). Moreover, it is highly likely that crystal fractionation involve assimilation of crustal materials (Stern and Gottfried, 1986).

5.2.1. Fractional crystallization

In this study, several petrographic and geochemical observations provide fundamental constraints on the petrogenesis of the Dokhan Volcanics, including: (1) the close spatial and temporal association of the different volcanic rock varieties suggest that these rocks are genetically related; (2) the systematic changes in mineralogy, especially the phenocryst assemblage; with increasing SiO_2 from the basalts to the rhyolites; (3) the general absence of textural and compositional evidence for disequilibrium, mixing, or contamination; (4) major and trace element abundances that vary along continuous trends of decreasing Al_2O_3, CaO, MgO, Fe_2O_3*, P_2O_5, TiO_2, Ni, and Sr and increasing K_2O, Rb, Nb, and Th

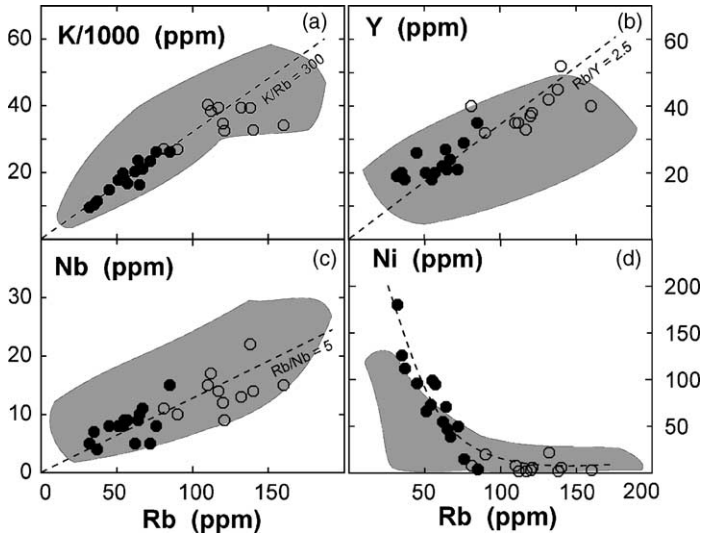

Fig. 8. Rb vs. K, Y, Nb, and Ni variation diagrams for the Dokhan Volcanic rocks in the South Safaga area (circles) and different areas in Egypt (shaded area). Notice the linear trends in incompatible (Rb) vs. incompatible (K, Y, and Nb) elements (a, b, and c) and curvilinear tends in incompatible (Rb) vs. compatible (Ni) elements (d). Symbols as in Fig. 2.

(Figs. 2 and 3) with increasing SiO_2; (5) incompatible (Rb) versus incompatible (K, Y, and Nb) trace element variations that are linear (Fig. 8a–c) with trends from low abundances in basalts towards higher abundances in rhyolites; (6) compatible (Ni) versus incompatible (Rb) trace elements variations form curved rather than linear trends (Fig. 8d); (7) the parallel nature of the normalized REE patterns (Fig. 4) with increasing total REE contents and decreasing Eu/Eu^* (measure of Eu anomalies) with increasing SiO_2 (Table 2); (8) La/Sm data points (Fig. 9a) plot along a horizontal line, a feature restricted to the process of fractional crystallization (Allegre and Minster, 1978).

The above-mentioned characteristics support previous suggestions that the Dokhan Volcanics evolved predominantly through fractional crystallization of the petrographically observed phenocryst assemblage, which is plagioclase + augite + hornblende + magnetite in the mafic volcanic rocks and plagioclase + K-feldspar + biotite + apatite + magnetite in the acidic varieties.

5.2.2. Crustal contamination

The chemical data of the Dokhan Volcanic rocks provide few constraints on whether or not there was significant crustal contamination, particularly because there is no data on the composition of the country rocks that may represent the potential contaminants. However, the LILE (e.g. Rb and K) and Zr are incompatible with respect to the major crystallizing phenocryst assemblage (plagioclase, augite, magnetite, and hornblende) and ratios like K/Rb and Rb/Zr do not significantly change by simple fractional crystallization of this assemblage. Variations in these ratios are preferably related to crustal contamination by assimilation fractional crystallization processes (Davidson et al., 1987). Examination of the Dokhan Volcanic rocks (Fig. 9b and c) shows that, in most of the samples of the intermediate volcanics, there is no significant variation in the K/Rb and Rb/Zr ratios. Therefore, the role of a significant crustal assimilation in the genesis of the intermediate Dokhan Volcanics is unlikely but cannot be completely ruled out. The recognition of ~680 Ma xenocrysts in andesite samples of the Dokhan Volcanics at the type locality area at Gebel Dokhan (Wilde and Youssef, 2000) support the idea of crustal contamination during evolution of these rocks. In the felsic volcanics, there are wider ranges in the K/Rb and Rb/Zr values, which indicate that significant contamination is involved at the very end of evolution of the entire volcanic suite.

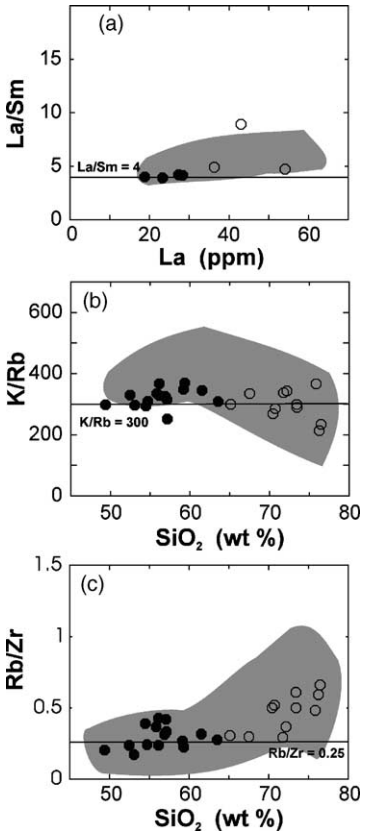

Fig. 9. La vs. La/Sm (a) and SiO_2 vs. K/Rb and Rb/Zr (b, c) for the Dokhan Volcanic rocks in the South Safaga area (circles) and different areas in Egypt (shaded area). Symbols as in Fig. 2.

6. Regional tectonic implications

The subduction processes (900–600 Ma) in the crustal evolution of the Arabian–Nubian Shield were terminated with the emplacement of calc-alkaline, collisional, I-type granitoids as follows: 640–610 Ma in Saudi Arabia (Fleck et al., 1980); 670–610 Ma in Egypt (Stern and Hedge, 1985); 615 Ma in Jordan (McCourt, 1990). At the very end of the late Neoproterozoic crustal evolution, a transition to extension tectonic regime occurred. Rock units diagnostic for such extensional tectonic regime in Egypt are the 610–550 Ma Dokhan Volcanic Group and the 600–585 Ma molasse-type Hammamat Group of sediments, which were intruded by post-orogenic A-type granites at 610–550 Ma (Stern and Hedge, 1985; Bentor, 1985; Sylvester, 1989; Beyth et al., 1994). Equivalent rock units in Saudi Arabia include the Shammar Group (600–555 Ma), which is widespread in the northern part of the Arabian Shield with a thickness of 1000–1400 m (Baubron et al., 1976; Hadley and Schmidt, 1980). It consists of undeformed post-orogenic volcanic rocks interbedded with coarse continental clastics, which indicate an alluvial to lacustrine environment of deposition and intruded by alkali granite at about 600–571 Ma (Baubron et al., 1976). In NE Sudan, the Amaki Series are late Neoproterozoic undeformed post-orogenic volcanic rocks and molasses-type sediments, which have a composition similar to the Dokhan Volcanics and the Hammamat Group in Egypt (Almond et al., 1984). In Jordan, The Hiayala volcaniclastic Formation and the Saramuj Conglomerate (595 Ma; Jarrar et al., 1993) are post-orogenic and have a composition similar to the Dokhan Volcanics and the Hammamat Group in Egypt (Jarrar et al., 1993). Therefor, the late Neoproterozoic post-orogenic extensional-related volcanic rocks are coeval with the formation of clastic basins at about 600 Ma all over the Arabian–Nubian Shield.

7. Conclusions

The Dokhan Volcanic suite in the South Safaga area includes two rock units, namely: (1) a mafic unit consisting of basalt, basaltic andesite, andesite, dacite and their pyroclastic equivalents and (2) a felsic unit of rhyodacite, rhyolite and welded tuffs (ignimbrite). This volcanic suite is spatially and temporally associated with clastic sediments and was emplaced into a deformed and metamorphosed volcano-sedimentary association and I-type tonalite–granodiorite intrusion. There are several petrographic and geochemical features indicating that the Dokhan Volcanics evolved predominantly through fractional crystallization of the observed phenocryst assemblage (plagioclase + augite + hornblende + magnetite in the mafic volcanics and plagioclase + K-feldspar + biotite + magnetite + zircon in the felsic volcanics). The role of a significant crustal assimilation in the genesis of the intermediate Dokhan Volcanics is unlikely but cannot be completely ruled out. In the felsic Dokhan Volcanics, the chemical data indicate that significant contamination is involved during their evolution.

The Dokhan Volcanics mark neither active subduction tectonic regime nor a true continental rift. The rocks were most probably produced by partial melting of a lithospheric mantle source during a collision-related extensional collapse event, which affected the crust during collisional stage (i.e. during the attachment of the accreted juvenile arc terranes to the East Saharan Craton in the west). The high-K calc-alkaline affinity as well as the LILE-enrichment and HFSE-depletion, which characterize the Dokhan Volcanics and are used as criteria for arc volcanics, are attributed to partial melting of metasomatized lithospheric mantle source.

Regional correlation indicates that the late Neoproterozoic extensional collapse event, during which the Dokhan Volcanics and associated clastic sediments formed, is a regional one. This event is broadly coeval with sedimentation of clastic materials similar to extensional-related deposits.

Acknowledgements

Field work is carried out with the help of the geologists of the Egyptian Geological Survey and Mining Authority to whom I am most grateful, especially Dr. R.I. Rifaei. Thanks are due to Prof. T. Andersen (Oslo University, Norway) for kindly doing the XRF analyses. I am also indebted to Prof. M.A. Hassanen (King Abdulaziz University) for help in doing REE analyses in Canada, and Prof. A.M. El Bouseily for numerous helpful comments during preparation of the article. Profs. R. Stern, U. Harms and A. Kröner are greatly acknowledged for their valuable and constructive reviews that greatly improved the manuscript.

References

Abdel-Rahman, A.M., 1996. Pan-African volcanism: petrology and geochemistry of the Dokhan Volcanic suite in the northern Nubian Shield. Geol. Mag. 133, 17–31.

Abdel-Rahman, A.M., Doig, R., 1987. The Rb–Sr geochronological evolution of the Ras Gharib segment of the northern Nubian Shield. J. Geol. Soc. London 144, 577–586.

Akaad, M.K., Noweir, A.M., 1980. Geology and lithostratigraphy of the Arabian Desert orogenic belt of Egypt between latitudes 25°35′S and 26°30′N. Inst. Appl. Geol. Jeddah Bull. 3, 127–135.

Almond, D.C., Ahmed, F., Dawoud, A.S., 1984. Tectonic, metamorphic and magnetic styles in the Northern Red Sea Hills of Sudan. Bull. Fac. Sci., King Abdulaziz Univ. Jeddah Bull. 6, 449–458.

Allegre, C.J., Minster, J.F., 1978. Quantitative models of trace element behaviour in magmatic processes. Earth Planet. Sci. Lett. 38, 1–25.

Atherton, M.P., Ghani, A.A., 2002. Slab breakoff: a model for Caledonian, Late Granite syn-collisional magmatism in the orthotectonic (metamorphic) zone of Scotland and Donegal. Ireland. Lithos 62, 65–85.

Basta, E.Z., Kotb, H., Awadalla, M.F., 1980. Petrochemical and geochemical characteristics of the Dokhan Formation at the type locality, Jabal Dokhan, Eastern Desert, Egypt. Inst. Appl. Geol. Jeddah Bull. 3, 121–140.

Baubron, J.C., Delfour, J., Vialette, Y., 1976. Geochronologic measurements (Rb/Sr, K/Ar) on rocks of the Arabian Shield, Kingdom of Saudi Arabia. Saudi Arabia Dir. Min. Res. Tech. Rep. 76-JED, 22, 152 pp.

Bentor, Y.K., 1985. The crustal evolution of the Arabo-Nubian Massif with special reference to the Sinai Peninsula. Precambrian Res. 28, 1–74.

Beyth, M., Stern, R.J., Altherr, R., Kröner, A., 1994. The late Precambrian Timna igneous complex, southern Israel: evidence for comagmatic-type sanukitoid monzodiorite and alkali granite magma. Lithos 31, 103–124.

Bird, P., 1979. Continental delamination and the Colorado Plateau. J. Geophys. Res. 84, 7561–7571.

Davidson, J.P., Ferguson, K.M., Colucci, M.T., Dungan, M.A., 1987. The origin of magmas from the San Pedro-Pellado Volcanic Dokhan Volcanics complex, S. Chile: multicomponent sources and open system evolution. Contrib. Mineral. Petrol. 100, 429–445.

Davies, J.H., von Blanckenburg, F., 1995. Slab breakoff: a model of lithospheric detachment and its test in the magmatism and delamination of collisional orogens. Earth Planet. Sci. Lett. 129, 85–102.

Dewey, J.F., 1984. Extensional collapse of orogens. Tectonics 7, 1123–1139.

El Bayoumi, R.M., Abu Zeid, H.T., Khalaf, E.A., 1997. Upper Proterozoic calc-alkaline and tholeiitic volcanics and their associates in the Gulf of Suez region, Egypt. Ann. Geol. Surv. Egypt 20, 125–142.

El Gaby, S., 1975. Petrochemistry and geochemistry of some granites from Egypt. Neus. Jahrb. Mineral. Abh. 124, 89–148.

El Gaby, S., List, F.K., Tehrani, R., 1988. Geology, evolution and metallogenesis of the Pan-African belt in Egypt. In: El Gaby, S., Greiling, R.O. (Eds.), The Pan-African Belt of Northeast Africa and Adjacent Areas. Braun, Schweig, Vieweg, pp. 17–68.

El Gaby, S., Khudeir, A.A., El Taky, M., 1989. The Dokhan Volcanics of Wadi Queih area, central Eastern Desert, Egypt. In: Proceedings of the 1st Conference on Geochemistry, Alexandria University, Egypt, pp. 42–62.

El Gaby, S., List, F.K., Tehrani, R., 1990. The basement complex of the Eastern Desert and Sinai. In: Said, R. (Ed.), The Geology of Egypt. Balkema Rotterdam, The Netherlands, pp. 175–184.

El Ramly, M.F., 1972. A new geological map for the basement rocks in the eastern and southwestern deserts of Egypt. Ann. Geol. Surv. Egypt 2, 1–18.

El Shazly, E.M., 1977. The geology of the Egyptian region. In: Narin, A.E., Kanes, W.H., Stehli, F.G. (Eds.), The Ocaen Basins and Margins, 4A, The Eastern Mediterranean. Plenum Press, New York, pp. 379–444.

El Sheshtawi, Y.A., El Tokhi, M.M., Ahmed, A.M., 1997. Petrogenesis of the Dokhan Volcanics of Wadi Dib and Wadi Abu Had, Esh El Mellaha, North Eastern Desert, Egypt. Ann. Geol. Surv. Egypt 20, 163–184.

Finger, F., Helmy, H.M., 1998. Composition and total-Pb model ages of monazite from high-grade paragneisses in the Abu Swayel area, south Eastern Desert, Egypt. Mineral. Petrol. 62, 269–289.

Fleck, R.J., Coleman, R.G., Cornwall, H.R., Greenwood, W.R., Hadley, D.G., 1976. Geochronology of the Arabian shield, western Saudi Arabia: K/Ar results. Geol. Soc. Am. Bull. 87, 9–21.

Fleck, R.J., Greenwood, W.R., Hadley, D.G., Andersen, R.E., Schmidt, D.L., 1980. Age and evolution of the southern part of the Arabian Shield. Instit. Appl. Geol. Jeddah Bull. 3, 1–17.

Francis, M.H., 1972. Geology of the basement complex of the North Eastern Desert between latitudes 27°30′S and 28°00′N. Ann. Geol. Surv. Egypt 2, 161–180.

Frisch, W., Abdel-Rahman, A.M., 1999. Petrogenesis of the Wadi Dib alkaline ring complex, Eastern Desert of Egypt. Mineral. Petrol. 65, 249–275.

Fritz, H., Wallbrecher, E., Khudeir, A.A., Abu El Ela, F.F., Dallmeyer, D.R., 1996. Formation of Neoproterozoic metamorphic core complexes during oblique convergence Eastern Desert, Egypt. J. Afr. Earth Sci. 23, 311–329.

Geological Map of Egypt, 1987. Scale 1:500,000. In: Klitsch, E., List, F.K., Pöhlmann, G. (Compil.), Conoco Coal and the Egyptian General Petroleum Corporation. Technische Fachhochschule, Berlin.

Ghobrial, M.G., Lotfi, M., 1967. The geology of Gabal Gattar and Gabal Dokhan areas. Geol. Surv. Egypt., Paper No. 40, 26 pp.

Gill, J., 1981. Orogenic Andesites and Plate Tectonics. Springer, Berlin, Heidelberg, New York, 390 pp.

Greiling, R.O., Abdeen, M.M., Dardir, A.A., El Akhal, H., El Ramly, M.F., Kamal El Din, G.M., Osman, A.F., Rashwan, A.A., Rice, A.H.N., Sadek, M.F., 1994. A structural synthesis of the Proterozoic Arabian–Nubian Shield in Egypt. Geol. Rundsch. 83, 484–501.

Grothaus, B., Eppler, D., Ehrlich, R., 1979. Depositional environments and structural implications of the Hammamat Formation. Egypt. Ann. Geol. Surv. Egypt 9, 564–590.

Hadley, D.G., Schmidt, D.L., 1980. Sedimentary rocks and basins of the Arabian Shield and their evolution. Instit. Appl. Geol. Jeddah Bull. 3, 25–50.

Hamilton, W.B., 1988. Plate tectonics and island arcs. Geol. Soc. Am. Bull. 100, 1503–1527.

Harms, U., Darbyshire, D.P.F., Denkler, T., Hengst, M., Schandelmeier, H., 1994. Evolution of the Neoproterozoic Delgo suture zone and crustal growth in Northern Sudan: geochemical and radiogenic isotope studies. Geol. Rundsch. 83, 591–603.

Hashad, A.H., 1980. Present status of geochronological data on the Egyptian basement complex. Instit. Appl. Geol. Jeddah Bull. 3, 31–46.

Hassan, M.A., Hashad, A.H., 1990. Precambrian of Egypt. In: Said, R. (Ed.), The Geology of Egypt. Balkema, Rotterdam, pp. 201–245.

Heikal, M.A., Higazy, M.H., El Rahmany, M.M., 1980. Ignimbritic rhyolite in the Wassif area, Eastern Desert, Egypt. Instit. Appl. Geol. Jeddah Bull. 3, 107–114.

Hume, W.F., 1935. Geology of Egypt, VII, Part II, The Later Plutonic and Minor Intrusive Rocks. Survey Egypt, Cairo.

Jarrar, G., Wachendorf, H., Zachmann, D., 1993. A Pan-African alkaline pluton intruding the Saramuj conglomerate, south-west Jordan. Geol. Rundsch. 82, 121–135.

Kröner, A., Reischmann, T., Wust, H.-J., Rashwan, A., 1988. Is there any pre-Pan-African (>950 Ma) basement in the Eastern Desert of Egypt? In: El Gaby, S., Greiling, R.O. (Eds.), The Pan-African Belt of Northeast Africa and Adjacent Areas. Braunschweig, Vieweg, pp. 93–119.

Kröner, A., Todt, W., Hussein, I.M., Mansour, M., Rashwan, A., 1992. Dating of late Proterozoic ophiolites in Egypt and the Sudan using single zircon evaporation technique. Precambrian Res. 59, 15–32.

Kröner, A., Krüger, J., Rashwan, A.A., 1994. Age and tectonic setting of granitoid gneisses in the Eastern Desert of Egypt and south-west Sinai. Geol. Rundsch. 83, 502–513.

Le Bas, M.J., Le Maitre, R.W., Streckeisen, A., Zanetin, B., 1986. A chemical classification of volcanic rocks based on the total alkalies-silica diagram. J. Petrol. 27, 745–750.

Mawas, S.G., 1986. Geological and geochemical studies on the area southwest of Safaga, Eastern Desert, Egypt. Unpublished Ph.D. thesis, Assiut University, Egypt, 212 pp.

McCourt, W.J., 1990. The geochemistry and tectonic setting of the granitic rocks and associated rocks in the Aqaba and Araba complexes of Southwest Jordan. Nat. Res. Auth. Bull. 10, 1–96.

Moghazi, A.M., 1994. Geochemical and radiogenic isotope studies of some basement rocks at the Kid area, southeastern Sinai, Egypt. Unpublished Ph.D. thesis, Alexandria University, Egypt, 377 pp.

Moghazi, A.M., 1999. Magma source and evolution of late Neoproterozoic granitoids in the Gabal El Urf area, Eastern Desert, Egypt: geochemical and Sr–Nd isotopic constraints. Geol. Mag. 136, 285–300.

Moghazi, A.M., 2002. Petrology and geochemistry of Pan-African granitoids, Kab Amiri area, Egypt: implications for tectono-magmatic stages in the Arabian–Nubian Shield evolution. Mineral. Petrol. 75, 41–67.

Moghazi, A.M., Andersen, T., Oweiss, G.A., El Bouseily, A.M., 1998. Geochemical and Sr–Nd–Pb isotopic data bearing on the origin of Pan-African granitoids in the Kid area, southeast Sinai, Egypt. J. Geol. Soc. London 155, 697–710.

Mohamed, F.H., Moghazi, A.M., Hassanen, M.A., 2000. Geochemistry, petrogenesis and tectonic setting of late Neoproterozoic Dokhan-type volcanic rocks in the Fatira area, eastern Egypt. Int. J. Earth Sci. 88, 764–777.

Neumann, E.R., Sundvoll, B., Overli, P.E., 1990. A mildly depleted upper mantle beneath southeast Norway: evidence from basalts in the Permo-Carboniferous Oslo rift. Tectonophysics 178, 89–107.

Pearce, J.A., Cann, J.R., 1973. Tectonic setting of basic volcanic rocks determined using trace element analyses. Earth Planet. Sci. Lett. 19, 290–300.

Pearce, J.A., Harris, N.B.W., Tindle, A.G., 1984. Trace element discrimination diagrams for the tectonic interpretation of granitic rocks. J. Petrol. 25, 956–983.

Peccerillo, A., 1985. Roman comagmatic province (central Italy): evidence for subduction-related magma geneses. Geology 13, 103–106.

Peccerillo, A., Taylor, S.R., 1976. Geochemistry of Eocene calc-alkaline volcanic rocks from the Kastamonu area, northern Turkey. Contrib. Mineral. Petrol. 58, 63–81.

Ragab, A.I., 1987. On the petrogenesis of the Dokhan Volcanics of the Northern Eastern Desert of Egypt. MERC Ain Shams Univ., Egypt, Earth Sci. Ser. 1, 151–158.

Ressetar, R., Monard, J.R., 1983. Chemical composition and tectonic setting of the Dokhan Volcanic formation, Eastern Desert, Egypt. J. Afr. Earth Sci. 1, 103–112.

Ries, A.C., Shackelton, R.M., Graham, R.H., Fitches, W.R., 1983. Pan-African structures, ophiolites and melange in the Eastern Desert of Egypt: a traverse at 26°N. J. Geol. Soc. London 140, 75–95.

Rock, N.M.S., 1984. Nature and origin of calc-alkaline lampophyres: minettes, vogesites, korsantites, and spessartites. Trans. Roy. Soc. Edinburgh 74, 193–227.

Rogers, N.W., Hawkesworth, C.J., 1985. The geochemistry of potassic lavas from Vulsini, central Italy, and implications for mantle enrichment processes beneath the Roman region. Contrib. Mineral. Petrol. 90, 244–257.

Rogers, N.W., Hawkesworth, C.J., Mattey, D.P., Harmon, R.S., 1987. Sediment subduction and the source of potassium in orogenic leucitites. Geology 15, 451–453.

Sacks, P.E., Secor, D.T., 1990. Delamination in collisional belts. Geology 18, 999–1002.

Schandelmeier, H., Richter, A., Harms, U., 1987. Proterozoic deformation of the East Saharan Craton in southeast Libya, south Egypt, and north Sudan. Tectonophysics 140, 233–246.

Shervais, J.W., 1982. Ti–V plots and the petrogenesis of modern ophiolitic lavas. Earth Planet. Sci. Lett. 59, 101–118.

Schürmann, H.M., 1966. The Precambrian Along the Gulf of Suez and the Northern Part of the Red Sea. EJ Bill Leiden, 404 pp.

Sloman, L.E., 1989. Triassic Shoshonites from the Dolomites, northern Italy, alkaline arc rocks in a strike–slip setting. J. Geophys. Res. 94, 4655–4666.

Stacey, J.S., Agar, R.A., 1985. U–Pb isotopic evidence for the accretion of a continental microplate in the Zalm region of the Saudi Arabian Shield. J. Geol. Soc. London 142, 1189–1204.

Stern, R.J., 1981. Petrogenesis and tectonic setting of late Precambrian ensimatic volcanic rocks, central Eastern Desert of Egypt. Precambrian Res. 16, 195–230.

Stern, R.J., 1994. Arc assembly and continental collision in the Neoproterozoic East African Orogen: implications for the consolidation of Gondwanaland. Ann. Rev. Earth Planet. Sci. 22, 319–351.

Stern, R.J., 2002. Crustal evolution in the East African Orogen: a neodymium isotopic prospective. J. Afr. Earth Sci. 34, 109–117.

Stern, R.J., Gottfried, D., 1986. Petrogenesis of late Precambrian (575–600 Ma) bimodal suite in northeast Africa. Contrib. Mineral. Petrol. 92, 492–501.

Stern, R.J., Hedge, C.E., 1985. Geochronologic and isotopic constraints on late Precambrian crustal evolution in the Eastern Desert of Egypt. Am. J. Sci. 285, 97–127.

Stern, R.J., Voegeli, D.A., 1987. Geochemistry, geochronology, and petrogenesis of a Late Precambrian (=590 Ma) composite dike from the North Eastern Desert of Egypt. Geol. Rundsch. 76, 325–341.

Stern, R.J., Gottfried, D., Hedge, C.E., 1984. Late Precambrian rifting and crustal evolution in the northeast Desert of Egypt. Geology 12, 168–172.

Stern, R.J., Sellers, G., Gottfried, D., 1988. Bimodal dyke swarms in the North Eastern Desert of Egypt: significance for the origin of late Precambrian "A-type" granites in northern Afro-Arabia. In: El Gaby, S., Greiling, R.O. (Eds.), The Pan-African Belt of Northeast Africa and Adjacent Areas. Vieweg, Weisbaden, pp. 147–177.

Sultan, M., Tucker, R.D., El Alfy, Z., Attia, R., Ragab, A.G., 1994. U–Pb (zircon) ages for the gneissic terrane west of the Nile, southern Egypt. Geol. Rundsch. 83, 514–522.

Sun, S.-S., 1982. Chemical composition and origin of the Earth's primitive mantle. Geochim. Cosmochim. Acta 46, 179–192.

Sun, S.-S., McDonough, W.E., 1989. Chemical and isotopic systematics of oceanic basalts: implications for mantle composition and processes. In: Saunders, A.D., Norry, M.J. (Eds.), Magmatism in the Oceanic Basins. Geol. Soc. Spec. Publ. 42, 313–345.

Sylvester, P.J., 1989. Post-collisional alkaline granites. J. Geol. 97, 261–280.

Thirwall, M.F., 1988. Wenlock to mid-Devonian volcanism of the Caledonian–Applachian Orogen. In: Harris, A.I., Fettes, D.J. (Eds.), The Caledonian–Applachian Orogen. Geol. Soc. London Spec. Publ. 38, 415–428.

Turner, S.P., Platt, J.P., George, R.M.M., Kelly, S.P., Pearson, D.G., Norwell, G.M., 1999. Magmatism associated with orogenic collapse of the Betic–Alboran Domain, S.E. Spain. J. Petrol. 40, 1011–1036.

Vail, J.R., 1985. Pan-African (Late Precambrian) tectonic terrains and the reconstruction of the Arabian–Nubian Shield. Geology 13, 839–842.

Wilde, S.A., Youssef, K., 2000. Significance of SHRIMP U–Pb dating of the imperial porphyry and associated Dokhan Volcanics, Gebel Dokhan, North Eastern Desert, Egypt. J. Afr. Earth Sci. 31, 403–413.

Willis, K.M., Stern, R.J., Clauer, N., 1988. Age and geochemistry of late Precambrian sediments of the Hammamat Series from the northeastern Desert of Egypt. Precambrian Res. 42, 173–187.

Wilson, M., 1989. Igneous Petrogenesis. Unwin Hyman, London, 457 pp.